Available online at www.sciencedirect.com
SCIENCE DIRECT
Nuclear Instruments and Methods in Physics Research B 242 (2006) 679–682
NIM B
Beam Interactions with Materials & Atoms
www.elsevier.com/locate/nimb

Monte-Carlo simulation study of the self-organization of nanometric amorphous precipitates in regular arrays during ion irradiation

F. Zirkelbach, M. Häberlen *, J.K.N. Lindner, B. Stritzker

Universität Augsburg, Institut für Physik, Universitätsstrasse 1, D-86135 Augsburg, Germany

Available online 10 October 2005

Abstract

High-dose ion implantation of materials that undergo drastic density change upon amorphization at certain implantation conditions results in periodically arranged, self-organized, nanometric configurations of the amorphous phase. A simple model explaining the phenomenon is introduced and implemented in a Monte-Carlo simulation code. Through simulation conditions for observing lamellar precipitates are specified and additional information about the compositional and structural state during the ordering process is gained.

PACS: 02.70.Uu; 61.72.Tt; 81.16.Rf

Keywords: Monte-Carlo simulation; Self-organization; Precipitation; Amorphization; Nanostructures; Ion irradiation

1. Introduction

Owing to the statistical nature of collision processes, ion implantation into solids leads first and foremost to disordered systems, such as depth profiles of different defects or distributions of precipitates with variable size. In the present paper we explore a self-organization process which leads to regular arrays of amorphous, lamellar nanoinclusions which have been observed for a number of ion/target combinations, e.g. O^+ or C^+ implantation into Si, Ar^+ into Al_2O_3 or Si^+ into SiC [1–3]. All these systems have in common that the amorphous phase has a largely reduced density of host atoms compared to the crystalline host lattice. Therefore the amorphous inclusions exert compressive stress on the host matrix, leading to their self-organized spacial arrangement. In the present work we focus on high-dose carbon implantations into silicon.

2. Mechanisms contributing to amorphization

High-dose carbon implantations performed at sufficiently high implantation temperatures to prevent complete surface amorphization and at the same time sufficiently low temperatures to prevent direct formation of crystalline 3C–SiC precipitates have been shown [4] to result in carbon-rich amorphous, nanometric precipitates (a-SiC_x). An example is presented in Fig. 1. Precipitation of carbon in an amorphous a-SiC_x phase saves the enormous interfacial energy [5] which would be required between crystalline 3C–SiC and c-Si due to a 20% lattice mismatch. Pure amorphous silicon (a-Si) is not stable against ion beam induced epitaxial recrystallization under the present implantation conditions [6] and therefore becomes stabilized by accumulation of carbon [7]. Vice versa, the fact that light C^+ ions can amorphize c-Si at these elevated temperatures is attributed to the presence of carbon impurities, the effect termed "carbon-induced amorphization" [8]. Once formed, a-SiC_x inclusions serve as diffusional sinks for excess carbon atoms in the c-Si phase (the room temperature solid solubility of C in c-Si being essentially zero). Since the Si atomic density of stoichiometric amorphous SiC is

* Corresponding author. Tel.: +49 821 5983498; fax: +49 821 5983425.
E-mail address: maik.haeberlen@physik.uni-augsburg.de (M. Häberlen).

0168-583X/$ - see front matter
doi:10.1016/j.nimb.2005.08.162

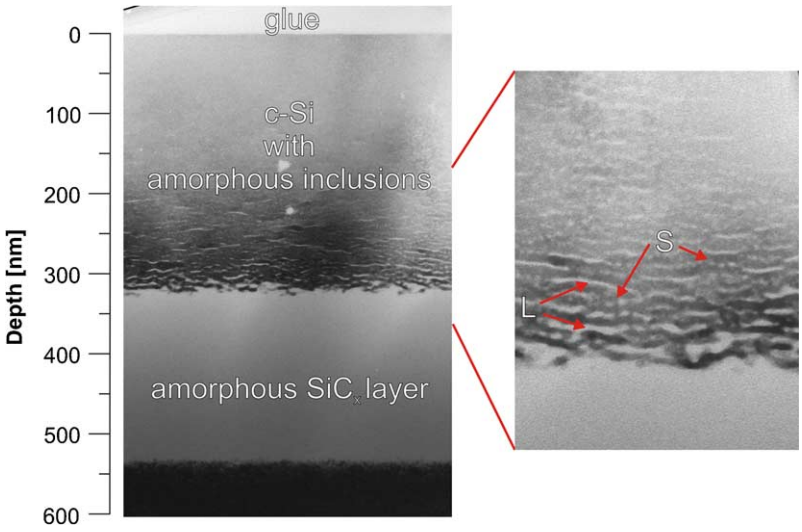

Fig. 1. Cross-sectional transmission electron microscopy (XTEM) image of a Si(1 0 0) sample implanted with 180 keV C^+ ions at a dose of 4.3×10^{17} cm^{-2} and a substrate temperature of 150 °C. Lamellar and spherical amorphous inclusions above a continuous amorphous layer are marked by L and S.

20–30% smaller than that of c-Si [9,10], a reduced density is also assumed for relaxed substoichiometric a-SiC$_x$. In the unrelaxed state a-SiC$_x$ inclusions are assumed to exert compressive stress on their surrounding which decays by a r^{-2} law. These stress fields enhance the local probability for further amorphization, as perfect crystal lattice restoration after an ion impact is less likely than in unstrained c-Si. This leads to the formation of amorphous lamellae by connecting the amorphous spheres laterally, as strain relaxation perpendicular to the surface can be easily achieved. In summary there are three main mechanisms contributing to amorphization: normal "ballistic" amorphization, carbon-induced amorphization and stress enhanced amorphization.

A simulation algorithm for amorphous volume generation/recrystallization including the above mechanisms has been proposed in [11]. In this article, the influence of stress-induced amorphization, carbon diffusion rate and carbon diffusion in z-direction are studied on the basis of simulations.

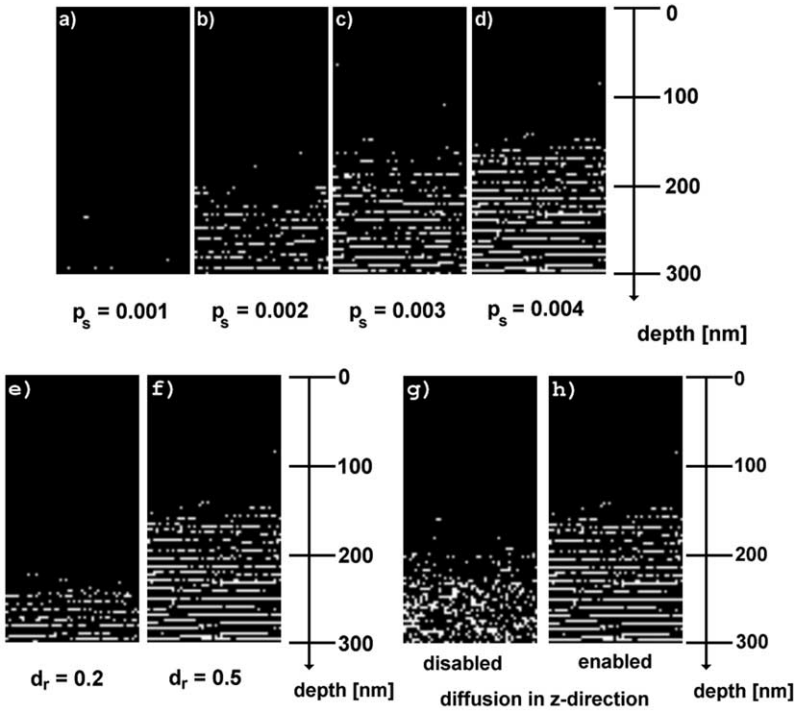

Fig. 2. Results of simulation runs (10^7 iterations) with increasing (a)–(d) stress influence (simulation parameter p_s), different diffusion rate d_r (e, f) and two runs with diffusion switched off (g) and on (h). In (e)–(h), $p_s = 0.004$.

3. Monte-Carlo simulation results

Results of simulation runs with different parameters are compared in Fig. 2. Black and white volumes represent crystalline and amorphous volumes in the relevant depth interval of 0–300 nm.

For otherwise identical simulation parameters, an increase in the influence of stress on the amorphization probability (Fig. 2(a)–(d)) leads to an increase of the amount of amorphous volumes and to more lamellar order.

The impact of carbon diffusion is shown in Fig. 2(e)–(h). Higher diffusion rates (Fig. 2(f)) result in larger depth domains of lamellar structure. This is due to the larger amount of carbon which is incorporated into amorphous volumes stabilizing the amorphous state even at low depth regions. In contrast, if carbon is less mobile (Fig. 2(e)), the redistribution of carbon is too slow to accumulate in carbon-rich amorphous volumes which are not affected by recrystallization. In particular, diffusion in z-direction is necessary to achieve an ordered lamellar structure, as is evident from Fig. 2(g) and (h), where lateral diffusion is as strong as in Fig. 2(f), and either enabled or disabled in z-direction. Amorphous volumes enhance their stability against recrystallization by depriving adjacent crystalline volumes of carbon. The probability of amorphization in a slice containing cells which are already amorphous is enhanced due to the stress resulting from carbon-rich amorphous precipitates. The amorphization in the carbon-denuded volumes and their lateral vicinity is decreased. This obviously fortifies the self-organization process.

As a consequence the amorphous and crystalline lamellae have a complementary arrangement in neighbouring layers m and $m+1$ as shown in Fig. 3(a) and (b). The carbon map in Fig. 3(c) and (d) verifies the carbon accumulation in the amorphous precipitates and the carbon-denuded crystalline area.

The compressive stress is visualized in Fig. 3(e) and (f). As expected, the location of the amorphous area corresponds to the location of high stress field, with the stress existing slightly beyond the amorphous precipitate.

A comparison of (a), (c) and (e) in Fig. 3 shows the different accounts for amorphization. Carbon-rich volumes are amorphous, effected by carbon-induced amorphization. Despite a decreased carbon concentration along the periphery of an amorphous lamella, amorphized volumes exceed the region of high carbon concentration due to additional compressive stress. Even volumes with nearly zero carbon concentration are still amorphous. At the c-Si side of amorphous/crystalline interfaces the remaining stress is not sufficiently large enough for amorphization.

Fig. 4 shows the carbon concentration in the amorphous and crystalline volumes for a simulation similar to the sample of Fig. 1. Up to a depth of 160 nm all the carbon is located in crystalline volumes as amorphous volumes do not exist. The linear increase of carbon concentration in this region results from the linearly approximated

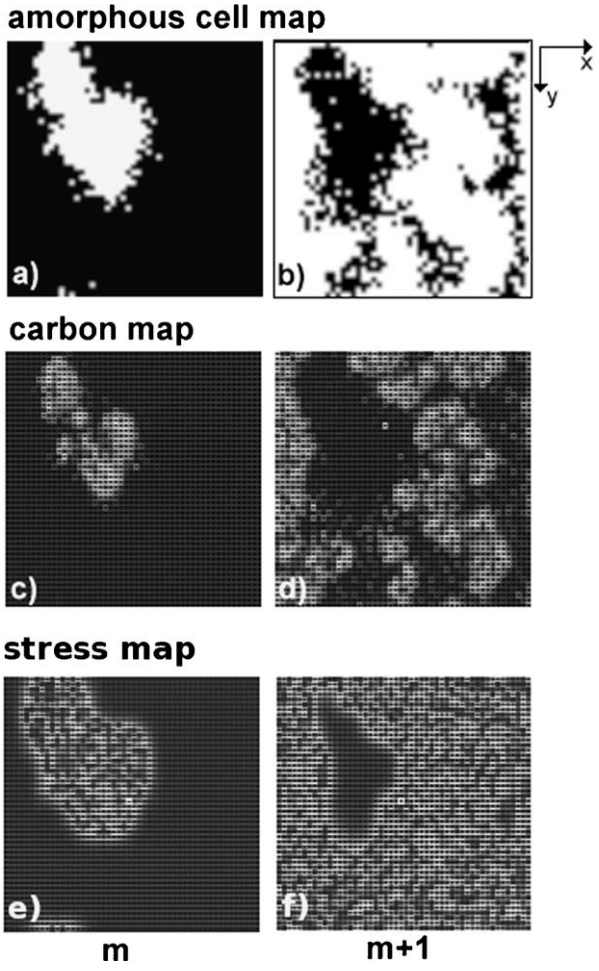

Fig. 3. Plane view display of amorphous (white) and crystalline (black) volumes in two consecutive layers m and $m+1$ (a, b) and corresponding carbon (c, d) and stress (e, f) map. Higher carbon concentrations and higher stresses are given by higher brightness in (c, d) and (e, f).

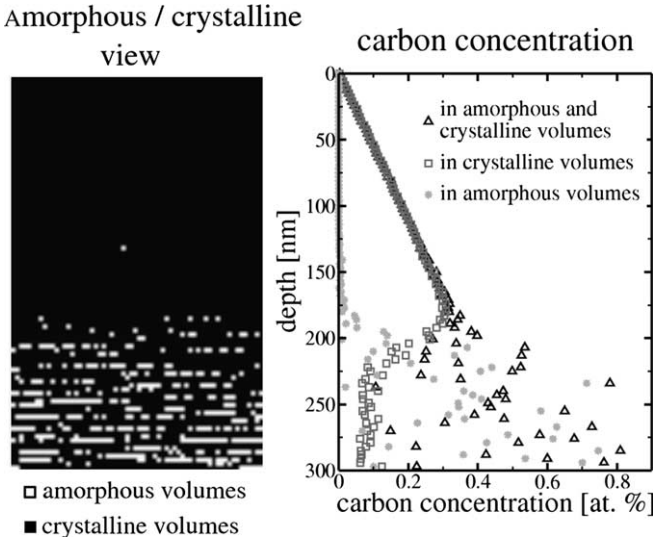

Fig. 4. Amorphous cell distribution and corresponding carbon implantation profile. The implantation profiles show the mean amount of carbon in amorphous and crystalline volumes as well as the sum for a dose of 0.81×10^{17} cm^{-2}.

implantation profile in the entire simulation window (0–300 nm). With starting amorphization carbon concentration is reduced in the crystalline phase while increased in the amorphous phase. The heavy carbon concentration fluctuations in the amorphous phase result from the changing number of carbon-accumulating amorphous precipitates in consecutive slices.

4. Summary and conclusions

A simple model explaining the self-organization process of amorphous, lamellar precipitates during high-dose ion implantation is proposed. A Monte-Carlo simulation based on this model is shown to be able to reproduce the experimentally observed formation of lamellar structures and makes the evolution traceable. Different mechanisms contributing to amorphization are studied by variation of corresponding simulation parameters. Diffusion and resulting accumulation of carbon in amorphous volumes together with carbon-induced and stress-induced amorphization are responsible for the formation of ordered arrays of amorphous lamellae. In the simulation, the influence of each of these mechanisms can be explored separately.

References

[1] L.L. Snead, S.J. Zinkle, J.C. Hay, M.C. Osborne, Nucl. Instr. and Meth. B 141 (1998) 123.
[2] A.H. van Ommen, Nucl. Instr. and Meth. B 39 (1989) 194.
[3] M. Ishimaru, R.M. Dickerson, K.E. Sickafus, Nucl. Instr. and Meth. B 166–167 (2000) 390.
[4] J.K.N. Lindner, M. Häberlen, M. Schmidt, W. Attenberger, B. Stritzker, Nucl. Instr. and Meth. B 186 (2002) 206.
[5] W.J. Taylor, T.Y. Tan, U. Gösele, Appl. Phys. Lett. 62 (1993) 3336.
[6] J. Linnross, R.G. Elliman, W.L. Brown, J. Mater. Res. 3 (1988) 1208.
[7] E.F. Kennedy, L. Csepregi, J.W. Mayer, J. Appl. Phys. 48 (1977) 4241.
[8] J.K.N. Lindner, B. Stritzker, Nucl. Instr. and Meth. B 147 (1999) 249.
[9] L.L. Horton, J. Bentley, L. Romana, A. Perez, C.J. McHargue, J.C. McCallum, Nucl. Instr. and Meth. B 65 (1992) 345.
[10] W. Skorupa, V. Heera, Y. Pacaud, H. Weishart, in: F. Priolo, J.K.N. Lindner, A. Nylandsted Larsen, J.M. Poate (Eds.), New Trends in Ion Beam Processing of Materials, Eur. Mater. Res. Soc. Symp. Proc. 65, Part 1, Elsevier, Amsterdam, 1997, p. 114.
[11] F. Zirkelbach, M. Häberlen, J.K.N. Lindner, B. Stritzker, Comp. Mater. Sci. 33 (2005) 310.